Geoscience Frontiers 4 (2013) 655–666

Contents lists available at SciVerse ScienceDirect

China University of Geosciences (Beijing)

Geoscience Frontiers

journal homepage: www.elsevier.com/locate/gsf

Research paper

Petrology and phase equilibrium modeling of sapphirine + quartz assemblage from the Napier Complex, East Antarctica: Diagnostic evidence for Neoarchean ultrahigh-temperature metamorphism

Hisako Shimizu [a], Toshiaki Tsunogae [a,b,*], M. Santosh [c,d]

[a] Graduate School of Life and Environmental Sciences, University of Tsukuba, Ibaraki 305-8572, Japan
[b] Department of Geology, University of Johannesburg, Auckland Park 2006, South Africa
[c] China University of Geosciences (Beijing), No. 29, Xueyuan Road, Haidian District, Beijing 100083, China
[d] Division of Interdisciplinary Science, Faculty of Science, Kochi University, Kochi 780-8520, Japan

ARTICLE INFO

Article history:
Received 7 July 2012
Received in revised form
30 August 2012
Accepted 20 September 2012
Available online 27 September 2012

Keywords:
Ultrahigh-temperature granulite
Petrology
Pseudosection modeling
Napier complex
Antarctica

ABSTRACT

A synthesis of the petrological characters of granulite facies rocks that contain equilibrium sapphirine + quartz assemblage from two localities (Tonagh Island (TI) and Priestley Peak (PP)) in the Napier Complex, East Antarctica, provides unequivocal evidence for extreme crustal metamorphism possibly associated with the collisional orogeny during Neoarchean. The reaction microstructures associated with sapphirine + quartz vary among the samples, probably suggesting different tectonic conditions during the metamorphic evolution. Sapphirine and quartz in TI sample were probably in equilibrium at the peak stage, but now separated by corona of Grt + Sil + Opx suggesting near isobaric cooling after the peak metamorphism, whereas the Spr + Qtz + Sil + Crd + Spl assemblage replaces garnet in PP sample suggesting post-peak decompression. The application of mineral equilibrium modeling in NCKFMASHTO system demonstrated that Spr + Qtz stability is lowered down to 930 °C due to small Fe^{3+} contents in the rocks (mole $Fe_2O_3/(FeO + Fe_2O_3) = 0.02$). The TI sample yields a peak *p-T* range of 950–1100 °C and 7.5–11 kbar, followed by cooling toward a retrograde stage of 800–950 °C and 8–10 kbar, possibly along a counterclockwise *p-T* path. In contrast, the peak condition of the PP sample shows 1000–1050 °C and >12 kbar, which was followed by the formation of Spr + Qtz corona around garnet at 930–970 °C and 6.7–7.7 kbar, suggesting decompression possibly along a clockwise *p-T* trajectory. Such contrasting *p-T* paths are consistent with a recent model on the structural framework of the Napier Complex that correlates the two areas to different crustal blocks. The different *p-T* paths obtained from the two localities might reflect the difference in the tectonic framework of these rocks within a complex Neoarchean subduction/collision belt.

© 2012, China University of Geosciences (Beijing) and Peking University. Production and hosting by Elsevier B.V. All rights reserved.

1. Introduction

The Napier Complex is known as a classic example of Neoarchean granulite terrane exposed around an area of ca. 300 km × 200 km in the Enderby Land of East Antarctica (e.g., Sheraton et al., 1987; Harley and Hensen, 1990; Boger, 2011; Horie et al., 2012; among others). The complex has excellent exposures of anhydrous granulites that were formed by deep crustal metamorphism at extreme thermal conditions of $T > 900$ °C and $p = 7–13$ kbar, referred to as ultrahigh-temperature (UHT) metamorphic rocks (e.g., Harley, 1985, 1998, 2008; Brown, 2007; Kelsey, 2008; Santosh and Kusky, 2010). The rocks formed through such UHT metamorphism, particularly at $T > 1000$ °C, are often characterized by the occurrence of several diagnostic minerals or mineral assemblages such as sapphirine + quartz, orthopyroxene + sillimanite + quartz, Al-rich

* Corresponding author. Graduate School of Life and Environmental Sciences, University of Tsukuba, Ibaraki 305-8572, Japan.
E-mail address: tsunogae@geol.tsukuba.ac.jp (T. Tsunogae).

Peer-review under responsibility of China University of Geosciences (Beijing).

Production and hosting by Elsevier

1674-9871/$ – see front matter © 2012, China University of Geosciences (Beijing) and Peking University. Production and hosting by Elsevier B.V. All rights reserved.
http://dx.doi.org/10.1016/j.gsf.2012.09.001

orthopyroxene, scapolite + wollastonite, mesoperthite, and inverted pigeonite (e.g., Harley, 1998; Harley and Motoyoshi, 2000; Hokada, 2001; Kelsey, 2008; and references therein; Tsunogae et al., 2011; Zhang et al., 2012). Among the assemblages of UHT metamorphism, sapphirine + quartz has been regarded as the most robust evidence for extreme temperatures, formed above 950 °C, and sometimes exceeding 1000 °C (e.g., Hensen and Green, 1973; Bertrand et al., 1991; Harley, 1998; Kelsey et al., 2004; Kelsey, 2008). The Amundsen Bay and Casy Bay areas, located in the western part of the Napier Complex, are regarded as the highest grade region of the complex, where sapphirine + quartz assemblages have been widely reported (e.g., Dallwitz, 1968; Ellis, 1980; Ellis et al., 1980; Grew, 1980, 1982; Motoyoshi and Matsueda, 1984; Sheraton et al., 1987; Motoyoshi and Hensen, 1989; Harley and Hensen, 1990; Osanai et al., 2001a,b; Tsunogae et al., 2002; Hokada et al., 2008; and references therein). The peak temperature conditions of $T > 1100$ °C or even >1150 °C have been suggested on the basis of the stability of sapphirine + quartz and related mineral assemblages as well as geothermometry (e.g., Harley et al., 1990; Harley and Motoyoshi, 2000; Hokada, 2001; Tsunogae et al., 2002). Recently Taylor-Jones and Powell (2010) reported lowering of the stability temperature of sapphirine + quartz assemblage down to 850 °C in highly oxidized states in FMASTO system and provided a new activity-composition (a–x) model for sapphirine that includes ferric iron. Similar lowering of the sapphirine + quartz stability temperature was reported by Korhonen et al. (2012) based on pseudosection analyses in KFMASHTO and NCKFMASHTO systems. Korhonen et al. (2012) suggested that the stability of sapphirine + quartz over a range of natural rock compositions should be investigated on a case-by-case basis using the modeling approach of chemical systems including Fe_2O_3. Although there are many sapphirine + quartz localities so far reported in the Napier Complex, and pseudosection approach has been tested to some of these sapphirine granulites (e.g., Hokada et al., 2008), no attempt has yet been made to evaluate the stability of sapphirine + quartz assemblage considering the effect of Fe_2O_3. In this study, we synthesize the petrographic and mineralogical characters of sapphirine + quartz from Tonagh Island and Priestley Peak in Amundsen Bay, and draw inferences on the *p-T* evolution of this area. We adopted mineral equilibrium technique in a complex chemical system including TiO_2 and Fe_2O_3 and evaluate the peak *p-T* condition of sapphirine + quartz assemblage from the localities. The sapphirine + quartz bearing assemblages from the two localities show distinct reaction textures that probably indicate different metamorphic evolution under different tectonic settings within the UHT orogen, possibly associated with subduction/collision events during Neoarchean.

2. General geology

The Amundsen Bay area in the Napier Complex is composed mainly of layered quartzo-feldspathic, pelitic, and psammitic gneisses with subordinate orthopyroxene-quartz-feldspar gneiss (charnockite or enderbite), mafic and ultramafic granulites, and magnetite quartzite (Sheraton et al., 1987). *p-T* estimates of the various lithologies from this region based on different methods such as conventional geothermometry (e.g., Ellis, 1980; Harley, 1985), phase analysis (e.g., Grew, 1980; Harley and Hensen, 1990; Harley et al., 1990; Harley, 1998), Al solubility in orthopyroxene (e.g., Harley and Motoyoshi, 2000), inverted pigeonite (e.g., Sandiford and Powell, 1986; Harley, 1987), oxygen isotope geothermometry (e.g., Farquhar et al., 1996), and ternary feldspar geothermometry (e.g., Hokada, 2001) suggest that the rocks were subjected to UHT metamorphism. The available geochronological data suggest that the granulite-facies peak metamorphism took place during Neoarchean to early Paleoproterozoic (ca. 2.5 Ga; e.g., Harley and Black, 1997; Carson et al., 2002; Hokada et al., 2003, 2004, 2008; Horie et al., 2012). The geological features of the locations examined in this study are summarized below.

2.1. Tonagh Island

Detailed regional geological framework and structural characteristics of Tonagh Island are given in Osanai et al. (2001a). Tonagh Island is dominantly composed of various metasedimentary and metaigneous rocks such as pelitic granulite, magnetite-quartzite (meta-BIF), mafic to ultramafic granulites, felsic garnet granulite, and felsic to intermediate orthopyroxene granulite (charnockite or enderbite). The rocks show dominant E–W trending foliation. The lithologies are divided into several blocks by E–W trending vertical shear zones. Mafic granulite and charnockite are dominant in the blocks in the north, whereas metasediments are abundant in the south. Peak metamorphic conditions of Tonagh Island were determined as $T > 1100$ °C using ternary-feldspar equilibrium (Hokada, 2001), phase equilibria on sapphirine granulites (Osanai et al., 1999), and Al solubility in orthopyroxene (Tsunogae et al., 2002). A counterclockwise *p-T* path has been proposed for the area based on geothermobarometry, phase analysis, and fluid inclusion study of Mg-Al rocks (Tsunogae et al., 2002).

A sapphirine + quartz bearing quartzo-feldspathic granulite from the eastern part of Tonagh Island was analyzed in this study. The lithology occurs as a thin (~30 cm) layer of garnet-pyroxene-rich brownish gray rock intercalated with felsic garnet gneiss, charnockite, quartzo-feldspathic sillimanite gneiss, and mafic granulite.

2.2. Priestley Peak

Priestley Peak is located about 10 km south of Tonagh Island (Fig. 1). No detailed field geological survey has been done so far in this locality. The studied area, which corresponds to the northwestern region of the exposure, is composed of layered gneisses of quartzo-feldspathic, mafic, and pelitic compositions, which are principally similar to the lithologies in the northern part of Tonagh Island. The analyzed sample of sapphirine granulite corresponds to a felsic layer within mafic to intermediate granulite.

3. Petrography and metamorphic reactions

Below we will summarize petrography and reaction textures related to sapphirine + quartz in the two localities described in the earlier section. The samples were collected during field geological survey of Amundsen Bay area undertaken by the 39th Japanese Antarctic Research Expedition (JARE-39) in 1998. Representative textures of the samples are shown in Figs. 2 and 3.

3.1. Sample B98021104AA (Tonagh Island)

The sample is composed of mesoperthite/perthite, quartz, garnet (Grt_1), sapphirine, and orthopyroxene (Opx_1). Sillimanite (Sil_1), ilmenite and rutile occur as accessory minerals. The rock shows weak foliation defined by quartzo-feldspathic layers and garnet-rich layers. Sapphirine, Opx_1, and Grt_1 occur as medium-grained subidioblastic minerals in the matrix of quartz and mesoperthite/perthite (Fig. 2a). Sil_1 occurs as needles or idioblasts only as inclusions in Grt_1 and sapphirine (Fig. 2a), probably as a prograde phase. The peak mineral assemblage of the rock is therefore inferred to be Kfs + Qtz + Grt_1 + Opx_1 + Spr + Ilm + Rt ± melt. The sapphirine is separated from quartz by corona of garnet (Grt_2), sillimanite (Sil_2), and orthopyroxene (Opx_2) (Figs. 2b, 3a and b). The width of Grt_2 + Sil_2 + Opx_2 coronae is 30–60 μm, and Sil_2 is always formed on the sapphirine side, while Grt_2 and Opx_2 on the quartz side (Fig. 3a and b). This texture suggests that

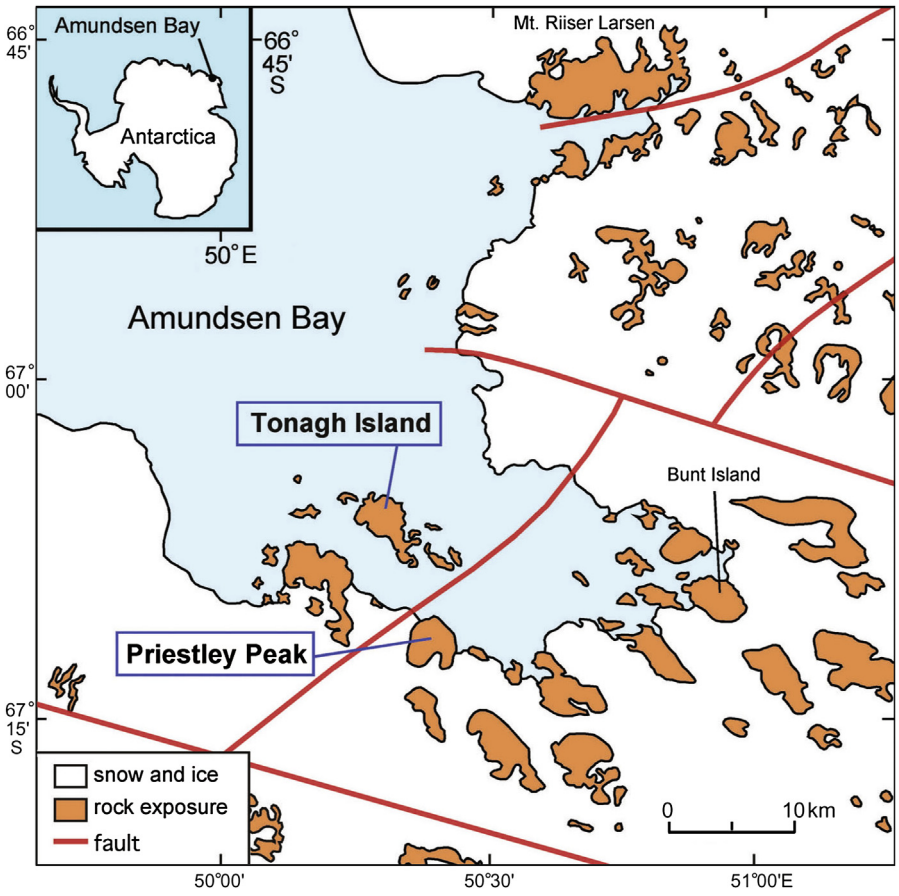

Figure 1. Location map of Tonagh Island and Priestley Peak in Amundsen Bay area, East Antarctica. Block boundaries are after Toyoshima et al. (2008).

sapphirine and quartz were once in equilibrium, but later separated by the progress of the following retrograde reaction (1).

$$Spr + Qtz \rightarrow Grt_2 + Sil_2 + Opx_2 \quad (1)$$

Similar reaction textures have been reported from several localities in the Napier Complex (e.g., Sheraton et al., 1987). The sapphirine is in places mantled by fine-grained aggregates of orthopyroxene (Opx_3), sillimanite (Sil_3), biotite, and quartz, suggesting the progress of further retrograde reaction (2) possibly with melt phase (Figs. 2c, 3c and d).

$$Spr + melt \rightarrow Opx_3 + Sil_3 + Bt + Qtz \quad (2)$$

3.2. Sample TS98022407 (Priestley Park)

The sample is composed of alternating quartzo-feldspathic and ferromagnesian layers. The quartzo-feldspathic layer is composed of mesoperthite/antiperthite, quartz, sapphirine, sillimanite, and garnet, while the ferromagnesian layer contains garnet, sillimanite, mesoperthite/antiperthite, quartz, sapphirine, spinel, cordierite, and rutile. Sapphirine (Spr_1) in the quartzo-feldspathic layer is xenoblastic, medium grained (0.2–0.5 mm), and often surrounded by plagioclase and K-feldspar (Figs. 2d and 3e), suggesting that Spr_1 is a prograde to peak phase. In contrast, in the ferromagnesian layer, sapphirine occurs as a retrograde mineral around garnet (Figs. 2e, 3f–h). As shown in Fig. 3f garnet is surrounded by aggregates of sapphirine (Spr_2) + sillimanite (Sil_2) + quartz + cordierite + spinel. Quartz is rare, but occurs as inclusions in Spr_2, and boundary between the Spr_2 and quartz is sharply defined. The probable peak assemblage in the ferromagnesian layer is inferred as garnet + Sil_1 + mesoperthite/antiperthite + quartz (Fig. 2f), which is coarse-grained and idioblastic to subidioblastic.

4. Mineral chemistry

Chemical analyses of all minerals were carried out using an electron microprobe analyzer (JEOL JXA8530F) at the Chemical Analysis Division of the Research Facility Center for Science and Technology, the University of Tsukuba. The analyses were performed under conditions of 15 kV accelerating voltage and 10 nA sample current, and the data were regressed using an oxide-ZAF correction program supplied by JEOL. Below we summarize the salient results from mineral chemistry data from the analyzed rocks. Representative compositions of minerals are given in Tables 1–3. Fe^{3+} of sapphirine and spinel was calculated based on stoichiometry.

4.1. Sapphirine

Sapphirine in the examined samples exhibits magnesian compositions (X_{Mg} = 0.81–0.85) close to the 7:9:3 ideal composition in terms of (Mg, Fe)O:Al_2O_3:SiO_2 ratio (Table 1, Fig. 4). For example, X_{Mg} range of subidioblastic sapphirine in B98021104AA (Tonagh Island; Fig. 3a) is 0.81–0.84. Spr_1 in sample TS98022407 (Priestley Peak) has consistent X_{Mg} of 0.81–0.85, and shows a slight rimward increase in X_{Mg} and $w(Cr_2O_3)$ content from 0.81–0.82 to 0.84–0.85 and from 1.1%–1.3% to 1.4%–1.5%, respectively. Retrograde

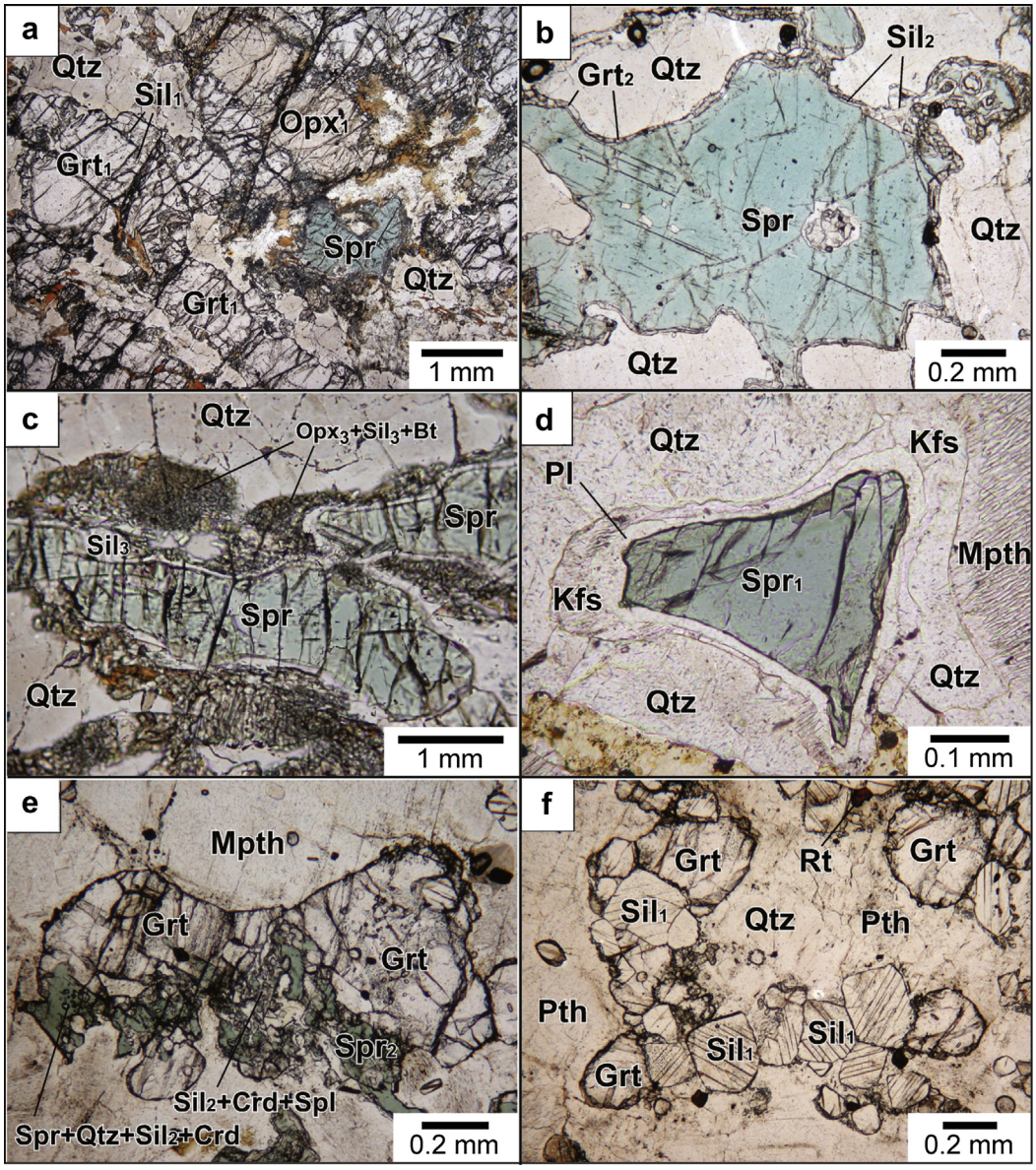

Figure 2. Photomicrographs showing reaction microstructures in sapphirine granulites discussed in this paper. Mineral abbreviations are discussed in the text. (a) to (c) are textures in sample B98021104AA (Tonagh Island), while (d) to (e) are in sample TS98022407 (Priestley Peak). All photographs are taken in polarized light. (a) Coarse-grained subidioblastic garnet, orthopyroxene, and quartz as a probable peak mineral assemblage. Sillimanite is present only as inclusions in garnet. Biotite occurs around the rim of some ferromagnesian minerals as a retrograde phase. Sapphirine is surrounded by reaction coronae as shown in Fig. 3b and c. (b) Corona of garnet + sillimanite between sapphirine and quartz, suggesting that sapphirine and quartz were once in equilibrium but subsequently separated by near isobaric cooling as discussed in the text. (c) Fine-grained symplectite of orthopyroxene + sillimanite + biotite between sapphirine and quartz probably related to a retrograde hydration event. (d) Subidioblastic sapphirine mantled by thin film of plagioclase and K-feldspar in quartz- and mesoperthite (Mpth)-rich portion of the rock. (e) Coronae of sillimanite + sapphirine + quartz and sillimanite + cordierite + spinel partly replacing prograde garnet, probably related to decompression during a retrograde stage. (f) Idioblastic to subidioblastic garnet + sillimanite + quartz + perthite as a probable peak mineral assemblage in garnet-rich layer of the rock.

Spr_2 shows consistent X_{Mg} of 0.83–0.84 and $w(Cr_2O_3)$ content of ~1.2%.

4.2. Garnet

Garnet in the samples is essentially a solid solution of pyrope and almandine (X_{Mg} = 0.51–0.58) with low grossular (<5 mol%) and spessartine (<2 mol%) contents (Table 2). It is compositionally nearly homogeneous, possibly due to diffusion during UHT metamorphism. In the Tonagh sample, matrix prograde Grt_1 and retrograde Grt_2 around sapphirine have nearly consistent compositions of $Alm_{48–52}$ $Pyr_{46–51}$ $Grs_{1–2}$ $Sps_{0–1}$ and Alm_{48} $Pyr_{50–51}$ Grs_1 $Sps_{0–1}$, respectively. Garnet in the Priestley Peak sample is slightly rich in pyrope component as $Alm_{41–45}$ $Pyr_{53–57}$ Grs_1 Sps_2.

4.3. Orthopyroxene

Three generations of orthopyroxene occur in sample B98021104AA. Subidioblastic coarse-grained orthopyroxene (Opx_1) has the highest $w(Al_2O_3)$ content of up to 7.6% (Al = 0.32 pfu) with X_{Mg} ratio of 0.74–0.77 (Table 2, Fig. 5). Opx_2 has lower $w(Al_2O_3)$ content (5.3%–5.5%, Al = 0.22–0.30 pfu) with consistent X_{Mg} ratio of 0.74–0.75. Symplectic Opx_3 shows the lowest X_{Mg} of 0.72 and intermediate $w(Al_2O_3)$ content of 6.5%–6.8% and Al = 0.27–0.29 pfu.

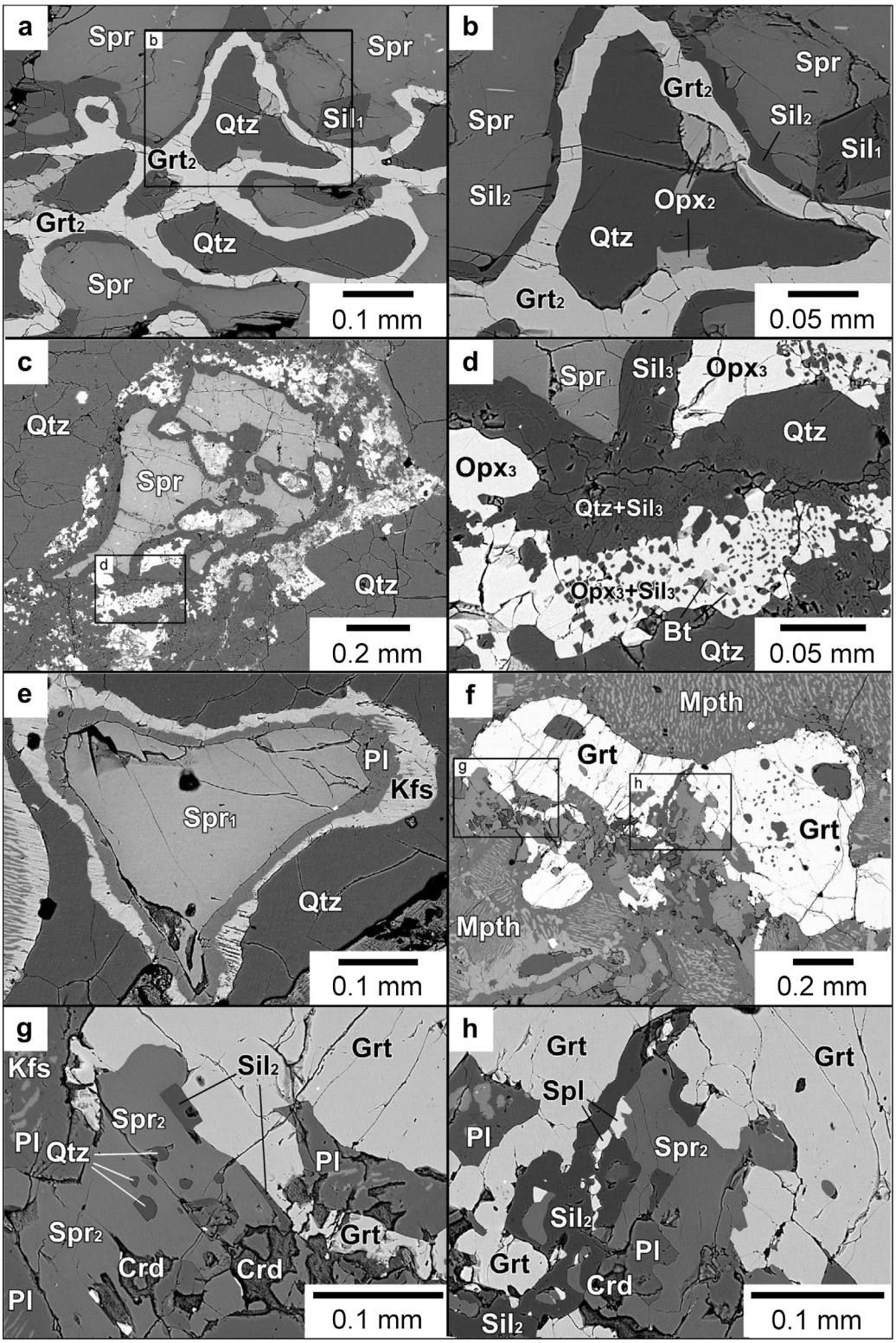

Figure 3. Back-scattered electron images showing detailed reaction microstructures in sample B98021104AA (Tonagh Island; Fig. 3a–d) and sample TS98022407 (Priestley Peak; Fig. 3e–h). (a), (b) Garnet + sillimanite + orthopyroxene corona between sapphirine + quartz. (c), (d) Orthopyroxene + sillimanite + biotite symplectite between sapphirine and quartz. (e) Subidioblastic sapphirine mantled by thin film of plagioclase and K-feldspar in quartz- and mesoperthite-rich portion of the rock. (f) Various corona textures in garnet probably related to decompression. (g) Sapphirine + quartz + sillimanite + cordierite corona around garnet. (h) Sillimanite + cordierite + spinel corona around garnet.

4.4. Other minerals

Spinel in sample TS98022407 (Priestley Peak) is Mg-rich (X_{Mg} = 0.59–0.66), and contains some Cr_2O_3 ($w(Cr_2O_3)$ = ~6.7%) and ZnO ($w(ZnO)$ = ~6.9%). The calculated $Fe^{3+}/(Fe^{2+} + Fe^{3+})$ ratio is low, 0.09–0.13. Plagioclase in TS98022407 occurs in several modes (lamella in mesoperthite, thin film around Spr_1, fine-grained phase with Spr_2 and Sil_2), but all of these show consistent

Table 1
Representative electron microprobe analyses of sapphirine, spinel, and sillimanite.

Mineral name	Sapphirine			Spinel	Sillimanite			
Sample Nos.	B98021104AA	TS98022407	TS98022407	TS98022407	B98021104AA	B98021104AA	TS98022407	TS98022407
O[a]	20	20	20	4	5	5	5	5
Remarks	Matrix	Spr_1	Spr_2		Sil_1	Sil_2	Sil_1	Sil_2
SiO_2	13.33	13.68	13.09	0.02	37.17	37.77	36.42	37.05
Al_2O_3	60.39	59.74	61.17	57.14	62.37	62.96	62.07	62.61
TiO_2	0.02	0.04	0.06	0.00	0.01	0.00	0.00	0.00
Cr_2O_3	0.26	1.27	1.17	6.71	0.01	0.04	0.17	0.08
Fe_2O_3	2.19	1.35	1.52	2.15	0.42	0.53	0.42	0.97
FeO	6.35	6.56	5.71	16.20				
MnO	0.04	0.10	0.03	0.02	0.06	0.01	0.03	0.00
MgO	16.49	16.53	16.77	13.01	0.01	0.05	0.03	0.09
ZnO	0.05	0.10	0.05	4.89	0.07	0.00	0.00	0.00
CaO	0.02	0.03	0.03	0.01	0.01	0.00	0.01	0.01
Na_2O	0.00	0.00	0.00	0.12	0.01	0.00	0.01	0.01
K_2O	0.00	0.02	0.01	0.00	0.02	0.02	0.01	0.00
Total	99.14	99.41	99.58	100.26	100.15	100.15	99.17	100.82
Si	1.605	1.645	1.564	0.000	1.002	1.007	0.992	0.991
Al	8.564	8.463	8.616	1.819	1.980	1.978	1.992	1.974
Ti	0.002	0.003	0.005	0.000	0.000	0.000	0.000	0.000
Cr	0.025	0.120	0.110	0.143	0.000	0.001	0.004	0.002
Fe^{3+}	0.199	0.122	0.136	0.044	0.008	0.011	0.009	0.020
Fe^{2+}	0.639	0.660	0.570	0.366				
Mn	0.004	0.010	0.003	0.000	0.001	0.000	0.001	0.000
Mg	2.957	2.961	2.986	0.524	0.001	0.001	0.001	0.003
Zn	0.004	0.009	0.004	0.098	0.001	0.000	0.000	0.000
Ca	0.002	0.004	0.004	0.000	0.000	0.000	0.000	0.000
Na	0.000	0.000	0.000	0.006	0.000	0.000	0.001	0.001
K	0.000	0.002	0.001	0.000	0.001	0.001	0.000	0.000
Total	14.000	14.000	14.000	3.000	2.996	2.998	2.998	2.991
$Mg/(Fe^{2+} + Mg)$	0.82	0.82	0.84	0.59				
$Zn/(Fe^{2+} + Mg + Zn)$				0.10				
$Fe^{3+}/(Fe^{3+} + Fe^{2+})$	0.24	0.16	0.19	0.11				

[a] Number of oxygens.

composition of Ab_{77-80}. K-feldspar in the sample is also nearly homogeneous in composition as Or_{86-92}. Sillimanite in the two samples is close to the ideal chemistry, but it sometimes contains small amount of Fe_2O_3 ($w(Fe_2O_3)$ = 0.32%–0.97%). Cordierite in sample B98022407 is Mg-rich as X_{Mg} = 0.89–0.90.

5. Mineral equilibrium modeling

Metamorphic *p-T* conditions of the stability of Spr + Qtz assemblages in the UHT granulites from Tonagh Island and Priestley Peak were constrained using THERMOCALC 3.33 (Powell and Holland, 1988, updated October 2009) with the internally consistent data set of Holland and Powell (1998; data set tcds55s, file created November 2003). The computations using this software are based on the stable mineral assemblage and phase compositions from Gibbs Free Energy minimization for a given bulk composition at specified *p-T* conditions, and the results are used to construct rock-specific equilibrium assemblage diagrams (also called pseudosections). Calculations were undertaken in the system Na_2O-CaO-K_2O-FeO-MgO-Al_2O_3-SiO_2-H_2O-TiO_2-Fe_2O_3 (NCKFMASHTO) (White et al., 2003, 2007), which provides a realistic approximation to model the examined rocks. The phases considered in the modeling and the corresponding *a–x* models used are garnet, biotite, and melt (White et al., 2007), orthopyroxene (White et al., 2002), plagioclase and K-feldspar (Holland and Powell, 2003), spinel and magnetite (White et al., 2002), sapphirine (Taylor-Jones and Powell, 2010), cordierite (Holland and Powell, 1998), and ilmenite-hematite (White et al., 2000). Aluminosilicates, quartz, and rutile are treated as pure end-member phases. For the analysis, slabs of relatively homogeneous part of the examined granulites were used for thin-section preparation, and the counterpart of these was used for chemical analysis. Bulk compositions for the rocks were determined by X-ray fluorescence spectroscopy and FeO/Fe_2O_3 ratio by titration at Activation Laboratories, Canada. The chemical composition of sample B98021104AA (Tonagh Island) is $w(SiO_2)$ = 68.06%, $w(Al_2O_3)$ = 12.67%, $w(FeO)$ = 6.70%, $w(MgO)$ = 8.41%, $w(MnO)$ = 0.027%, $w(CaO)$ = 0.14%, $w(Na_2O)$ = 0.04%, $w(K_2O)$ = 0.72%, $w(TiO_2)$ = 0.60%. Fe_2O_3 is taken into account for the calculations because the rock contains 0.43% of $w(Fe_2O_3)$, which we regard not negligible. Sample TS98022407 (Priestley Peak) shows slightly Al-rich composition of $w(SiO_2)$ = 57.20%, $w(Al_2O_3)$ = 23.74%, $w(Fe_2O_3)$ = 0.14%, $w(FeO)$ = 3.50%, $w(MgO)$ = 2.92%, $w(MnO)$ = 0.047%, $w(CaO)$ = 2.09%, $w(Na_2O)$ = 4.94%, $w(K_2O)$ = 3.52%, $w(TiO_2)$ = 0.77%. Analysis of the Priestley Peak sample was done on the ferromagnesian layer of the sample to infer the stability of sapphirine + quartz.

5.1. Tonagh Island

Sample B98021104AA contains Kfs + Qtz + Grt_1 + Spr + Opx_1 + Ilm + Rt ± inferred melt, representing the probable peak assemblage as discussed in the petrography section. Fig. 6a shows a *p-T* pseudosection for the sample calculated using the compositional factors listed in Fig. 6 a and at mole H_2O ratio of the rock ($M(H_2O)$) of 0.2 mol%. The stability field of the peak mineral assemblage of the rock plotted in the pseudosection suggests a *p-T* range of 950–1100 °C and 7.5–11 kbar for the assemblage. The upper *p-T* stability limit of the assemblage is defined by the absence of K-feldspar, whereas the lower limit is set by the absence of sapphirine. Spr + Qtz has a minimum stability field of 940 °C and 7 kbar, although at the condition, Spr + Qtz should coexist with cordierite, which is not the case of this rock. If we adopted higher $M(H_2O)$ values such as 1.0 mol% (Fig. 6b), the minimum stability of Spr + Qtz slightly increases as >950 °C and >7 kbar, but the stability field of the peak mineral

Table 2
Representative electron microprobe analyses of garnet, orthopyroxene, cordierite, and biotite.

Mineral name	Garnet					Orthopyroxene				Cordierite	Biotite
Sample	B98021	B98021	TS980	TS980		B98021	B98021	B98021	B98021	TS980	B98021
Nos.	104AA	104AA	22407	22407		104AA	104AA	104AA	104AA	22407	104AA
O[a]	12	12	12	12		6	6	6	6	18	22
Remarks	Grt_1	Grt_2	Core	Rim		Opx_1, core	Opx_1, rim	Opx_2	Opx_3		
SiO_2	40.25	41.03	40.64	40.95		51.95	51.38	51.61	51.33	49.57	40.42
Al_2O_3	22.89	23.03	23.15	23.48		7.56	6.93	6.99	6.50	33.74	14.08
TiO_2	0.03	0.00	0.01	0.03		0.07	0.05	0.05	0.00	0.00	3.72
Cr_2O_3	0.00	0.00	0.07	0.13		0.04	0.01	0.05	0.00	0.01	0.00
FeO[b]	22.81	22.82	21.21	20.66		14.34	14.50	15.60	17.10	2.61	5.96
MnO	0.07	0.10	0.28	0.37		0.05	0.02	0.00	0.05	0.06	0.00
MgO	13.55	13.37	14.96	14.80		26.12	26.26	25.34	24.99	12.10	20.81
ZnO	0.00	0.05	0.00	0.00		0.00	0.00	0.01	0.17	0.00	0.00
CaO	0.59	0.45	0.66	0.58		0.00	0.03	0.00	0.02	0.01	0.01
Na_2O	0.00	0.00	0.00	0.00		0.02	0.02	0.00	0.02	0.04	0.19
K_2O	0.00	0.00	0.00	0.00		0.00	0.00	0.00	0.01	0.01	9.74
Total	100.19	100.19	100.97	101.00		100.14	99.20	99.64	100.18	98.15	94.93
Si	3.001	3.033	2.988	2.999		1.851	1.853	1.860	1.856	4.960	5.785
Al	2.011	2.005	2.005	2.026		0.317	0.294	0.297	0.277	3.978	2.375
Ti	0.002	0.000	0.000	0.002		0.002	0.001	0.001	0.000	0.000	0.400
Cr	0.000	0.000	0.004	0.007		0.001	0.000	0.001	0.000	0.001	0.000
Fe^{2+}	1.421	1.410	1.303	1.265		0.427	0.437	0.470	0.517	0.197	0.713
Mn	0.004	0.006	0.018	0.023		0.002	0.000	0.000	0.001	0.005	0.000
Mg	1.504	1.472	1.638	1.615		1.386	1.410	1.360	1.346	1.804	4.436
Zn	0.000	0.003	0.000	0.000		0.000	0.000	0.000	0.004	0.000	0.000
Ca	0.047	0.036	0.052	0.045		0.000	0.001	0.000	0.001	0.001	0.001
Na	0.000	0.000	0.000	0.000		0.001	0.001	0.000	0.001	0.007	0.052
K	0.000	0.000	0.000	0.000		0.000	0.000	0.000	0.000	0.002	1.778
Total	7.992	7.992	8.008	7.982		3.988	3.999	3.990	4.005	10.955	15.542
Mg/(Fe + Mg)	0.51	0.51	0.56	0.56		0.76	0.76	0.74	0.72	0.90	0.86
Pyr (%)	50.5	50.3	54.4	54.8	X_{Al}[c]	0.16	0.15	0.15	0.14		
Alm (%)	47.7	48.2	43.3	42.9	y(Opx)[c]	0.17	0.15	0.16	0.13		
Grs (%)	1.6	1.2	1.7	1.5							
Sps (%)	0.1	0.2	0.6	0.8							

[a] Number of oxygens.
[b] Total Fe as FeO.
[c] $X_{Al} = Al/2$, $y(Opx) = Si + Al - 2$.

assemblage is not available at the H_2O content, as the stability field of Kfs shifts to lower temperature, while melt phase increases the stability field. Therefore, M(H_2O) value during the peak metamorphism should be lower than 1.0 mol%, which is consistent with the dry mineral assemblage during the peak metamorphism.

As the peak Spr + Qtz assemblage is replaced by $Grt_2 + Sil_2 + Opx_2$ corona formed by the progress of reaction (1), we regard that the *p-T* condition shifted toward the stability of Grt + Sil + Opx without sapphirine. The stability field of the inferred assemblage (Grt + Opx + Sil + Kfs + Ilm + Rt + Qtz + Liq) is 800–950 °C and 8–10 kbar, suggesting near isobaric cooling from the peak stage to form the retrograde assemblage.

5.2. Priestley Peak

The ferromagnesian layer of sample TS98022407 contains the probable peak assemblage of Grt + Kfs + Qtz + Pl + Sil + Qtz + Rt ± inferred melt as discussed previously. Fig. 7a shows a *p-T* pseudosection for the sample calculated using the compositional factors listed in Fig. 7a and at M(H_2O) = 0.2 mol%. The stability field of the assemblage occurs at $p > 12$ kbar and $T = 1000–1050$ °C. The upper-*T* stability limit of the assemblage is defined by the occurrence of K-feldspar while the lower-*T* limit is defined by the lack of spinel. As garnet in the sample is replaced by aggregates of $Spr_2 + Sil_2$ + Qtz + Crd + Spl, the metamorphic condition of the rock should have shifted to the stability of the assemblage, which corresponds to the stability field of Grt + Kfs + Qtz + Pl + Spr + Sil + Spl + Crd + Rt in Fig. 7a at 6.7–7.7 kbar and 930–970 °C within the stability field of sapphirine + quartz. We constructed a pseudosection at higher M(H_2O) values such as 1.0 mol%, which is shown in Fig. 7b. However, the stability field of the peak mineral assemblage is absent at such high water content, as the stability field of Kfs shifts to lower temperature, while the stability of melt phase expands toward higher temperature. Therefore, M(H_2O) value during the peak metamorphism is inferred to be lower than 1.0 mol%.

6. Discussion

6.1. UHT metamorphism in the Napier Complex

This study examined the stability of Spr + Qtz assemblage from two localities in the Napier Complex based on phase equilibrium approach in NCKFMASHTO system and confirmed that the mineral assemblage was stable at the peak UHT metamorphism of $T = 950–1100$ °C (Tonagh Island) and 930–970 °C (Priestley Peak). Although there are several reports on Spr + Qtz from the Napier Complex (e.g., Dallwitz, 1968; Ellis et al., 1980; Grew, 1980; Sheraton et al., 1987; Harley, 1998, 2004, 2008; Osanai et al., 2001a; Tsunogae et al., 2002, 2008; Hokada et al., 2008), this is the first attempt to apply pseudosection approach in a complex system including TiO_2 and Fe_2O_3. Earlier phase equilibrium studies placed the stability of Spr + Qtz at $T > 1030$ °C and $p = 9.5$ kbar (Hensen and Green, 1973) or $T > 1050$ °C and 11 kbar (Bertrand et al., 1991). Recent thermodynamic modeling in the KFMASH system also supports the high-temperature stability of this assemblage

Table 3
Representative electron microprobe analyses of feldspars.

Mineral name	K-feldspar		Plagioclase		
Sample Nos.	B980-21 104AA	TS980-22407	TS980-22407	TS980-22407	TS980-22407
O[a]	8	8	8	8	8
Remarks		Around Spr_1	Around Spr_1	With Kfs	In Spr
SiO_2	63.86	64.91	62.54	63.69	62.98
Al_2O_3	18.75	18.91	22.57	22.78	22.99
TiO_2	0.04	0.00	0.01	0.00	0.04
Cr_2O_3	0.02	0.00	0.01	0.00	0.00
FeO[b]	0.05	0.04	0.09	0.00	0.13
MnO	0.02	0.02	0.00	0.00	0.05
MgO	0.01	0.00	0.01	0.00	0.00
ZnO	0.00	0.00	0.05	0.02	0.00
CaO	0.03	0.27	4.61	3.77	4.25
Na_2O	1.43	1.70	9.06	8.74	8.95
K_2O	15.17	13.95	0.10	0.20	0.23
Total	99.37	99.81	99.06	99.20	99.62
Si	2.969	2.982	2.796	2.826	2.796
Al	1.027	1.023	1.189	1.191	1.203
Ti	0.001	0.000	0.000	0.000	0.001
Cr	0.001	0.000	0.000	0.000	0.000
Fe^{2+}	0.002	0.002	0.003	0.000	0.005
Mn	0.001	0.001	0.000	0.000	0.002
Mg	0.000	0.000	0.001	0.000	0.000
Zn	0.000	0.000	0.002	0.001	0.000
Ca	0.002	0.013	0.221	0.179	0.202
Na	0.129	0.152	0.785	0.752	0.770
K	0.899	0.817	0.006	0.011	0.013
Total	5.030	4.991	5.004	4.960	4.992
An (%)	0.2	1.4	21.8	19.0	20.5
Ab (%)	12.5	15.4	77.6	79.8	78.1
Or (%)	87.3	83.2	0.6	1.2	1.3

[a] Number of oxygens.
[b] Total Fe as FeO.

(T > 1005 °C, Kelsey et al., 2004; Kelsey, 2008). Our results demonstrated that the Spr + Qtz stability of the samples is lowered down to 940 °C (Tonagh Island) and 930 °C (Priestley Peak) at $M(H_2O) = 0.2$ mol.% due to small Fe^{3+} contents in the rocks (mole $Fe_2O_3/(FeO+Fe_2O_3) = 0.02$ and 0.03, respectively), which is consistent with the observations by Taylor-Jones and Powell (2010) and Korhonen et al. (2012). The results of our mineral equilibrium modeling on sapphirine granulites therefore conformed lowering of Spr + Qtz stability by addition of minor components such as Fe_2O_3 and TiO_2. The high geothermal gradient estimated from the peak p-T conditions (30–40 °C/km) provides unequivocal evidence for the formation of extreme metamorphic rocks within Amundsen Bay area of the Napier Complex possibly associated with the Neoarchean orogenic event.

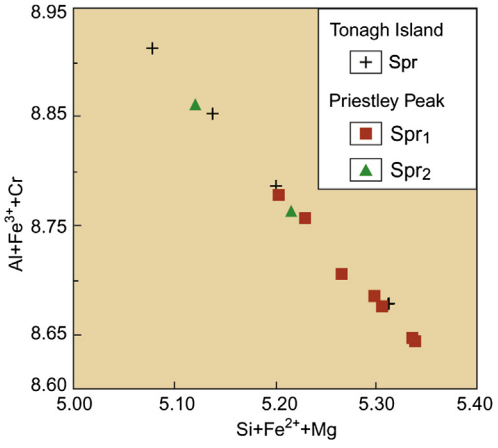

Figure 4. A compositional diagram showing sapphirine chemistry.

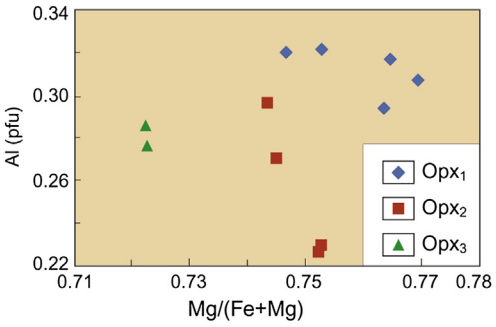

Figure 5. A compositional diagram showing orthopyroxene chemistry.

6.2. Implications for p-T evolution of the Napier Complex

Although the occurrences of Spr + Qtz assemblages in granulites from the two localities in the Napier Complex suggest peak UHT metamorphism, reaction microstructures related to the diagnostic UHT assemblage discussed in this study indicate two contrasting p-T trajectories: near-isobaric cooling and near-isothermal decompression. $Sil_2 + Grt_2 + Opx_2$ corona between sapphirine and quartz in sample B98021104AA from Tonagh Island is consistent with cooling from ca. 1000 °C to <950 °C at nearly consistent pressure of 8–10 kbar possibly along a counterclockwise p-T path (Fig. 6a). Such a counterclockwise p-T path has been reported from Tonagh Island by Tsunogae et al. (2002) on the basis of fluid inclusion analysis. Corona texture of Grt + Qtz after Cpx + Pl in mafic granulites from Tonagh Island (Tsunogae et al., 1999) as well as other localities (e.g., Ellis and Green, 1985; Harley, 1985; Sheraton et al., 1987) also supports isobaric cooling of Tonagh Island. In contrast, $Spr_2 + Qtz + Sil_2 + Crd + Spl$ corona around garnet in sample TS98022407 from Priestley Peak suggests decompression from >12 kbar and 1000–1050 °C to 6.7–7.7 kbar and 930–970 °C toward the stability field of Spr + Qtz along a clockwise p-T path. Such a clockwise p-T evolution of the studied region is consistent with previous studies on Bunt Island (e.g., Osanai et al., 2001b) located about 25 km east from Priestley Peak.

Macroscopic structural study of the Napier Complex by Toyoshima et al. (2008) suggested that the Napier Complex is separated into at least two types of metamorphic units or crustal bocks by fault/shear zones; clockwise p-T block (Block-1) and counterclockwise p-T block (Block-2). Block-1 is characterized by the occurrence of peak Opx + Sil assemblage and retrograde osumilite and cordierite in Mg-Al and pelitic granulites, that are indicative of clockwise p-T path. On the other hand, granulites in Block-2 contain Opx + Grt or Opx + Sil coronae between sapphirine and quartz, suggesting that sapphirine and quartz were once in equilibrium, but then corona was formed by near-isobaric cooling possibly along a counterclockwise p-T path. According to the classification of Toyoshima et al. (2008), our studied localities are separated by a major crustal break (Amundsen Bay Fault) as shown in Fig. 1, and Tonagh Island belongs to Block-2, while Priestley Peak is a part of Block-1. As discussed previously, the sapphirine granulite from Tonagh Island discussed in this study contains $Sil_2 + Grt_2 + Opx_2$ corona between sapphirine and quartz, which suggests near isobaric cooling from the stability of Spr + Qtz (ca. 1000 °C) to <950 °C at 8–10 kbar possibly along a counterclockwise

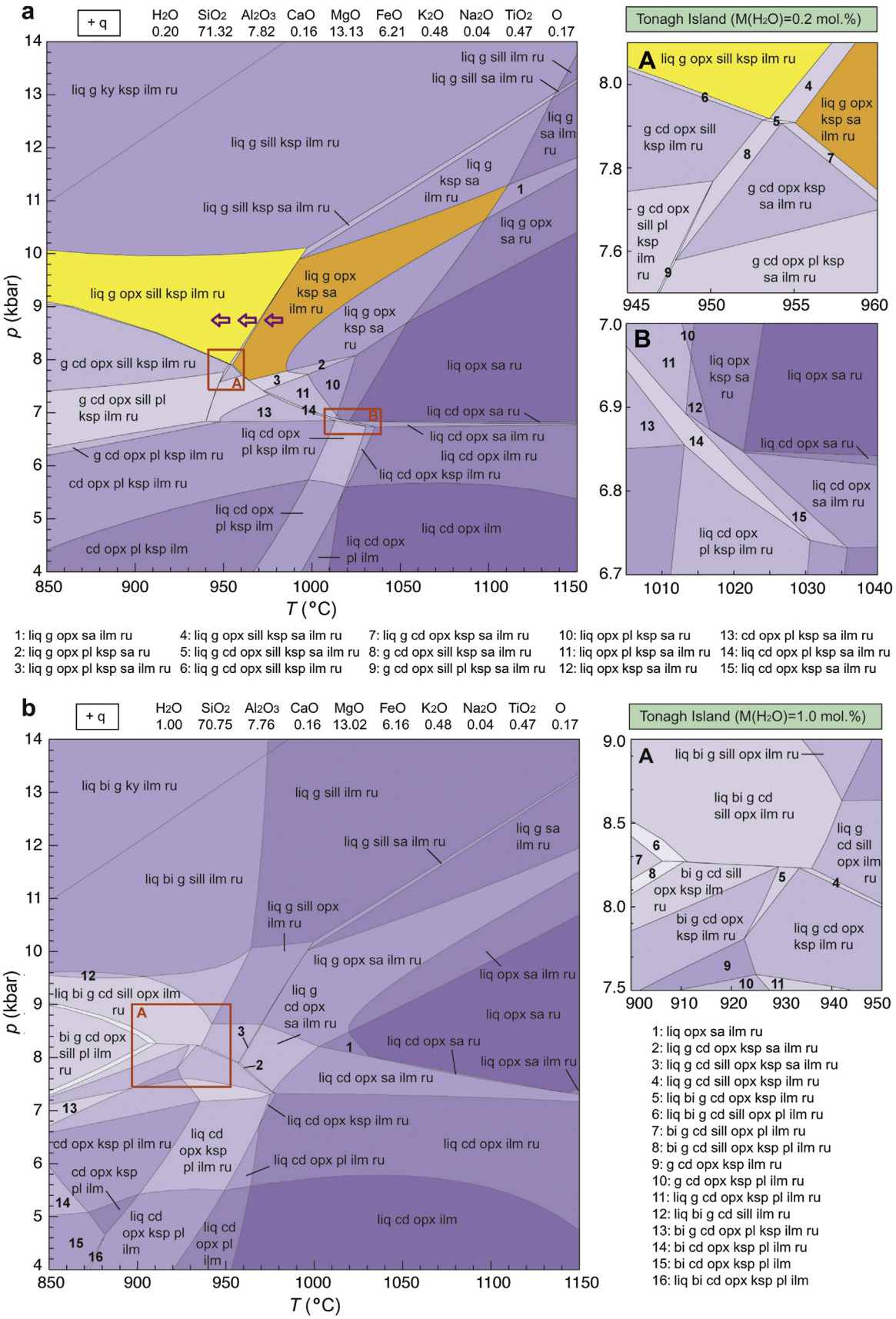

Figure 6. *p-T* diagrams showing calculated pseudosections of mineral assemblages in sample B98021104AA from Tonagh Island at M(H_2O) = 0.2 mol% (a) and M(H_2O) = 1.0 mol% (b). Hatched areas in (a) show peak and retrograde mineral assemblages. q: quartz, pl: plagioclase, ksp: K-feldspar, g: garnet, opx: orthopyroxene, sa: sapphirine, bi: biotite, sill: sillimanite, ky: kyanite, sp: spinel, cd: cordierite, mt: magnetite, ilm: ilmenite, ru: rutile, liq: inferred melt.

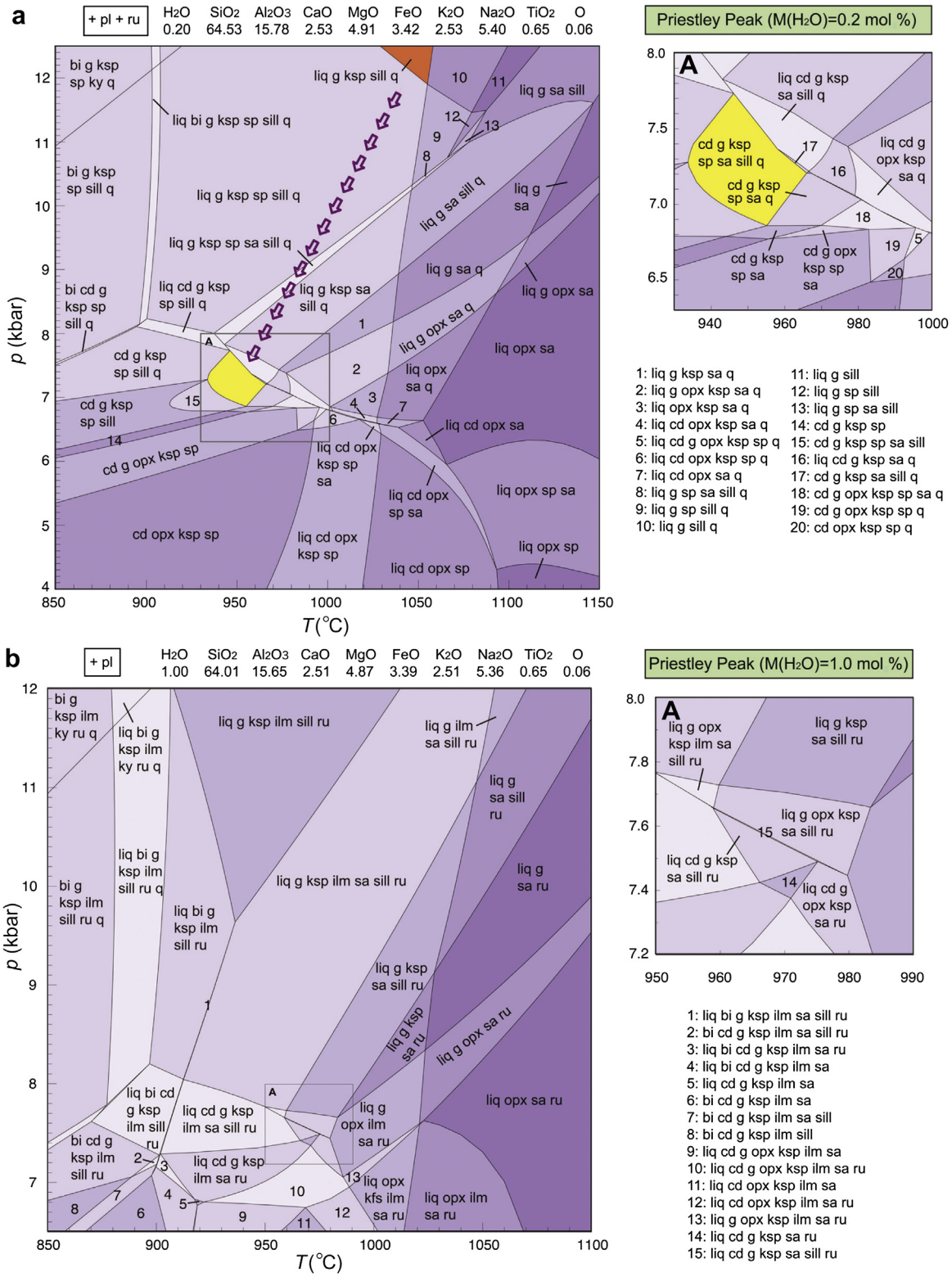

Figure 7. *p-T* diagrams showing calculated pseudosections of mineral assemblages in sample TS98022407 from Priestley Peak at M(H_2O) = 0.2 mol% (a) and M(H_2O) = 1.0 mol% (b). Hatched areas show peak and retrograde mineral assemblages.

p-T path (Fig. 6a). On the other hand, Spr + Qtz corona around garnet from Priestley Peak suggests decompression along clockwise *p-T* history, which is a unique character for Block-1. The results of our *p-T* paths based on pseudosection approach on Spr + Qtz granulite in NCKFMASHTO system therefore support the model that the Amundsen Bay area in the Napier Complex is composed of discrete crustal blocks that contain contrasting *p-T* histories.

The different *p-T* paths obtained from different rock units within a single metamorphic complex are common in many subduction-accretion-collision belts in the world. For example, in the Neoproterozoic–Cambrian Southern Granulite Terrane in India, isobaric cooling from very high-*T* condition or possible counter-clockwise *p-T* path is inferred from sapphirine granulites in the Madurai Block (e.g., Santosh and Sajeev, 2006; Tsunogae and Santosh, 2006, 2010), whereas prograde high-pressure and peak ultrahigh-temperature metamorphisms along a clockwise *p-T* path have been illustrated for mafic granulites and Mg-Al-rich rocks from adjacent Palghat-Cauvery Suture Zone (e.g., Shimpo et al., 2006; Collins et al., 2007; Nishimiya et al., 2010). Santosh et al. (2009) interpreted the evolution of the Southern Granulite Terrane through a model involving a progressive sequence from Pacific-type subduction-accretion orogeny to Himalayan-type collisional orogeny. This model envisages the Madurai Block as a long-lived Neoproterozoic magmatic arc with accretionary belts and exhumed hot orogens, and regarded such isobaric cooling along a possible counterclockwise *p-T* path inferred from the Madurai Block as a result of input of heat related to magmatic underplating. In contrast, the clockwise *p-T* evolution through high-pressure and UHT metamorphism within the Palghat-Cauvery Suture Zone reflects deep subduction of supracrustal materials, which were metamorphosed and extruded during the final continent-continent collisional stage. Although detailed tectonic framework of the Napier Complex is not known due to limited rock exposure as well as complete recrystallization of the rocks at peak UHT stage, the different *p-T* paths obtained from the two localities might reflect the difference in the tectonic framework of these rocks within the complex subduction/collision belt. Further detailed petrological, structural, and geochronological investigations on the UHT granulites are necessary to fully understand the evolution of Neoarchean orogenic event in the Napier Complex.

7. Concluding remarks

Although the occurrence of equilibrium sapphirine + quartz assemblage from several localities in the Neoarchean Napier Complex, East Antarctica, provides unequivocal evidence for regional UHT metamorphism, the reaction microstructures associated with sapphirine + quartz from two localities (Tonagh Island and Priestley Peak) suggest different tectonic evolution within the complex. Petrography and mineral equilibrium modeling in NCKFMASHTO system suggest that sapphirine and quartz in Tonagh Island sample are separated by corona of Grt + Sil + Opx suggesting near isobaric cooling after the peak metamorphism (from 950–1100 °C and 7.5–11 kbar to 800–950 °C and 8–10 kbar) possibly along a counterclockwise *p-T* path, whereas the Spr + Qtz + Sil + Crd + Spl assemblage replaces garnet in Priestley Peak sample suggesting post-peak decompression (from 1000–1050 °C and >12 kbar to 930–970 °C and 6.7–7.7 kbar) possibly along a clockwise *p-T* trajectory. Such contrasting *p-T* paths are consistent with a recent model on the structural framework of the Napier Complex that correlates the two areas to different crustal blocks. The different *p-T* paths obtained from the two localities might reflect the difference in the tectonic framework of these rocks within a complex Neoarchean subduction/collision belt.

Acknowledgments

We express our sincere thanks to the members of JARE-39 and the crew of the icebreaker Shirase for giving us the opportunity for geological field investigation of the Napier Complex, and for their helpful support. Especially we thank Professors Y. Osanai, T. Toyoshima, M. Owada, K. Shibuya, K. Moriwaki, K. Shiraishi, Y. Motoyoshi, Drs. T. Hokada, and W. Crowe for their field support and discussion. Shimizu thanks Drs. Fawna J. Korhonen and Chris Clark for their guidance of pseudosection calculations. Dr. N. Nishida is acknowledged for his assistance on microprobe analyses. Drs. C.V. Dharma Rao and Shoujie Liu provided valuable comments and suggestions to the earlier version of this manuscript. We thank these reviewers as well as Prof. Xiaoqiao Wan for his editorial comments. Partial funding for this project was produced by a Grant-in-Aid for Scientific Research (B) from Japan Society for the Promotion of Science (JSPS) to Tsunogae (Nos. 20340148, 22403017) and a Grant-in-Aid for JSPS Fellows to Shimizu (No. 23-311).

References

Bertrand, P., Ellis, D.J., Green, D.H., 1991. The stability of sapphirine-quartz and hypersthene-sillimanite-quartz assemblages: an experimental investigation in the system FeO-MgO-Al_2O_3-SiO_2 under H_2O and CO_2 conditions. Contributions to Mineralogy and Petrology 108, 55–71.

Boger, S.D., 2011. Antarctica – before and after Gondwana. Gondwana Research 19, 335–371.

Brown, M., 2007. Metamorphism, plate tectonics, and the supercontinent cycle. Earth Science Frontiers 14, 1–18.

Carson, C.J., Ague, J.J., Coath, C.D., 2002. U–Pb geochronology from Tonagh Island, East Antarctica: implications for the timing of ultra-high temperature metamorphism of the Napier Complex. Precambrian Research 116, 237–263.

Collins, A.S., Clark, C., Sajeev, K., Santosh, M., Kelsey, D.E., Hand, M., 2007. Passage through India: the Mozambique ocean suture, high-pressure granulites and the Palghat-Cauvery Shear System. Terra Nova 19, 141–147.

Dallwitz, W.B., 1968. Co-existing sapphirine and quartz in granulite from Enderby Land, Antarctica. Nature 219, 476–477.

Ellis, D.J., 1980. Osumilite-sapphirine-quartz granulites from Enderby Land, Antarctica: *P–T* conditions of metamorphism, implications for garnet-cordierite equilibria and the evolution of the deep crust. Contributions to Mineralogy and Petrology 74, 201–210.

Ellis, D.J., Green, D.H., 1985. Garnet-forming reactions in mafic granulites from Enderby Land, Antarctica – implications for geothermometry and geobarometry. Journal of Petrology 26, 633–662.

Ellis, D.J., Sheraton, J.W., England, R.N., Dallwitz, W.B., 1980. Osumilite-sapphirine-quartz granulites from Enderby Land, Antarctica: mineral assemblages and reactions. Contributions to Mineralogy and Petrology 72, 123–143.

Farquhar, J., Chacko, T., Ellis, D.J., 1996. Preservation of oxygen isotope compositions in granulites from Northwestern Canada and Enderby Land, Antarctica: implications for high-temperature isotopic thermometry. Contributions to Mineralogy and Petrology 125, 213–224.

Grew, E.S., 1980. Sapphirine + quartz association from Archean rocks in Enderby Land, Antarctica. American Mineralogist 65, 821–836.

Grew, E.S., 1982. Osumilite in the sapphirine–quartz terrane of Enderby Land, Antarctica: implications for osumilite petrogenesis in the granulite facies. American Mineralogist 67, 762–787.

Harley, S.L., 1985. Garnet-orthopyroxene bearing granulites from Enderby Land, Antarctica: metamorphic pressure–temperature–time evolution of the Archean Napier Complex. Journal of Petrology 26, 819–856.

Harley, S.L., 1987. A pyroxene-bearing meta-ironstone and other pyroxene-granulites from Tonagh Island, Enderby Land, Antarctica: further evidence for very high temperature (>980 °C) Archaean regional metamorphism in the Napier Complex. Journal of Metamorphic Geology 5, 341–356.

Harley, S.L., 1998. Special Publication. On the Occurrence and Characterization of Ultrahigh-temperature Crustal Metamorphism, vol. 138. Geological Society, London, pp. 81–107.

Harley, S.L., 2004. Extending our understanding of ultrahigh-temperature crustal metamorphism. Journal of Mineralogical and Petrological Sciences 99, 140–158.

Harley, S.L., 2008. Refining the *P–T* records of UHT crustal metamorphism. Journal of Metamorphic Geology 26, 125–154.

Harley, S.L., Black, L.P., 1997. A revised Archaean chronology for the Napier Complex, Enderby Land, from SHRIMP ion-microprobe studies. Antarctic Science 9, 74–91.

Harley, S.L., Hensen, B.J., 1990. Archaean and Proterozoic high-grade terranes of East Antarctica (40–80°E): a case study of diversity in granulite facies metamorphism. In: Ashworth, J.R., Brown, M. (Eds.), High-temperature Metamorphism and Crustal Anatexis. Kluwer Academic Publishers, pp. 320–370.

Harley, S.L., Motoyoshi, Y., 2000. Al zoning in orthopyroxene in a sapphirine quartzite: evidence for >1120 °C UHT metamorphism in the Napier Complex, Antarctica, and implications for the entropy of sapphirine. Contributions to Mineralogy and Petrology 138, 293–307.

Harley, S.L., Hensen, B.J., Sheraton, J.W., 1990. Two-stage decompression in orthopyroxene-sillimanite granulites from Forefinger Point, Enderby Land, Antarctica: implications for the evolution of the Archaean Napier Complex. Journal of Metamorphic Geology 8, 591–613.

Hensen, B.J., Green, D.H., 1973. Experimental study of the stability of cordierite and garnet in pelitic compositions at high pressures and temperatures. III. Synthesis of experimental data and geological applications. Contributions to Mineralogy and Petrology 38, 151–166.

Hokada, T., 2001. Feldspar thermometry in ultrahigh-temperature metamorphic rocks: evidence of crustal metamorphism attaining ~1100 °C in the Archean Napier Complex, East Antarctica. American Mineralogist 86, 932–938.

Hokada, T., Misawa, K., Shiraishi, K., Suzuki, S., 2003. Mid to late Archaean (3.3–2.5 Ga) tonalitic crustal formation and high-grade metamorphism at Mt. Riiser-Larsen, Napier Complex, East Antarctica. Precambrian Research 127, 215–228.

Hokada, T., Misawa, K., Yokoyama, K., Shiraishi, K., Yamaguchi, A., 2004. SHRIMP and electron microprobe chronology of UHT metamorphism in the Napier Complex, East Antarctica: implications for zircon growth at >1,000 °C. Contributions to Mineralogy and Petrology 147, 1–20.

Hokada, T., Motoyoshi, Y., Suzuki, S., Ishikawa, M., Ishizuka, H., 2008. Geodynamic evolution of Mt. Riiser Larsen, Napier Complex, East Antarctica, with reference to the UHT mineral associations and their reaction relations. Geological Society, London, Special Publications, vol. 308, pp. 253–282.

Holland, T.J.B., Powell, R., 1998. An enlarged and update internally consistent thermodynamic dataset with uncertainties and correlations: the system K_2O-Na_2O-CaO-MgO-MnO-FeO-Fe_2O_3-Al_2O_3-TiO_2-SiO_2-C-H_2-O_2. Journal of Metamorphic Geology 8, 89–124.

Holland, T.J.B., Powell, R., 2003. Activity-composition relations for phases in petrological calculations: an asymmetric multicomponent formulation. Contributions to Mineralogy and Petrology 145, 492–501.

Horie, K., Hokada, T., Hiroi, Y., Motoyoshi, Y., Shiraishi, K., 2012. Contrasting Archaean crustal records in western part of Napier Complex, East Antarctica: new constraints from SHRIMP geochronology. Gondwana Research 21, 829–837.

Kelsey, D.E., 2008. On ultrahigh-temperature crustal metamorphism. Gondwana Research 13, 1–29.

Kelsey, D.E., White, R.W., Holland, T.J.B., Powell, R., 2004. Calculated phase equilibria in K_2O-FeO-MgO-Al_2O_3-SiO_2-H_2O for sapphirine-quartz-bearing mineral assemblages. Journal of Metamorphic Geology 22, 559–578.

Korhonen, F.J., Powell, R., Stout, J.H., 2012. Stability of sapphirine + quartz in the oxidized rocks of the Wilson Lake terrane, Labrador: calculated equilibria in NCKFMASHTO. Journal of Metamorphic Geology 30, 21–36.

Motoyoshi, Y., Hensen, B.J., 1989. Sapphirine-quartz-orthopyroxene symplectites after cordierite in the Archaean Napier Complex, Antarctica: evidence for a counterclockwise *P–T* path? European Journal of Mineralogy 1, 467–471.

Motoyoshi, Y., Matsueda, H., 1984. Archaean granulites from Mt. Riiser-Larsen in Enderby Land, East Antarctica. Memoir of National Institute of Polar Research, Special Issue 33, pp. 103–125.

Nishimiya, Y., Tsunogae, T., Santosh, M., 2010. Sapphirine + quartz corona around magnesian (X_{Mg} ~0.58) staurolite from the Palghat-Cauvery Suture Zone, southern India: evidence for high-pressure and ultrahigh-temperature metamorphism within the Gondwana suture. Lithos 114, 490–502.

Osanai, Y., Toyoshima, T., Owada, M., Tsunogae, T., Hokada, T., Crowe, W.A., 1999. Geology of ultrahigh-temperature metamorphic rocks from Tonagh Island in the Napier Complex, East Antarctica. Polar Geoscience 12, 1–28.

Osanai, Y., Toyoshima, T., Owada, M., Tsunogae, T., Hokada, T., Yoshimura, Y., Miyamoto, T., Motoyoshi, Y., Crowe, W.A., Harley, S.L., Kanao, M., Iwata, M., 2001a. Explanatory Text of Geological Map of Tonagh Island, Enderby Land, Antarctica. Antarctic Geological Map Series (Sheet 38). National Institute of Polar Research, Japan.

Osanai, Y., Toyoshima, T., Owada, M., Tsunogae, T., Hokada, T., Crowe, W.A., Kusachi, I., 2001b. Ultrahigh temperature sapphirine-osumilite and sapphirine-quartz granulites from Bunt Island in the Napier Complex, East Antarctica: reconnaissance estimation of *P–T* evolution. Polar Geoscience 14, 1–24.

Powell, R., Holland, T.J.B., 1988. An internally consistent thermodynamic dataset with uncertainties and correlations: 3. Application, methods, worked examples and a computer program. Journal of Metamorphic Geology 6, 173–204.

Sandiford, M., Powell, R., 1986. Pyroxene exsolution in granulites from Fyfe Hills, Enderby Land, Antarctica: evidence for 1000 °C metamorphic temperatures in Archean continental crust. American Mineralogist 71, 946–954.

Santosh, M., Kusky, T., 2010. Origin of paired high pressure–ultrahigh-temperature orogens: a ridge subduction and slab window model. Terra Nova 22, 35–42.

Santosh, M., Sajeev, K., 2006. Anticlockwise evolution of ultrahigh-temperature granulites within continental collision zone in southern India. Lithos 92, 447–464.

Santosh, M., Maruyama, S., Sato, K., 2009. Anatomy of a Cambrian suture in Gondwana: Pacific-type orogeny in southern India? Gondwana Research 16, 321–341.

Sheraton, J.W., Tingey, R.J., Black, L.P., Offe, L.A., Ellis, D.J., 1987. Geology of an unusual Precambrian high-grade metamorphic terrane – Enderby Land and western Kemp Land, Antarctica. BMR Bulletin 223, 51.

Shimpo, M., Tsunogae, T., Santosh, M., 2006. First report of garnet-corundum rocks from Southern India: implications for prograde high-pressure (eclogite-facies?) metamorphism. Earth and Planetary Science Letters 242, 111–129.

Taylor-Jones, K., Powell, R., 2010. The stability of sapphirine + quartz: calculated phase equilibria in FeO-MgO-Al_2O_3-SiO_2-TiO_2-O. Journal of Metamorphic Geology 28, 615–633.

Toyoshima, T., Osanai, Y., Nogi, Y., 2008. Special Publications. Macroscopic geological structures of the Napier and Rayner Complexes, East Antarctica. Geological Society of London, vol. 308, pp. 139–146.

Tsunogae, T., Santosh, M., 2006. Spinel-sapphirine-quartz bearing composite inclusion within garnet from an ultrahigh-temperature pelitic granulite: implications for metamorphic history and *p–T* path. Lithos 92, 524–536.

Tsunogae, T., Santosh, M., 2010. Ultrahigh-temperature metamorphism and decompression history of sapphirine granulites from Rajapalaiyam, southern India: implications for the formation of hot orogens during Gondwana assembly. Geological Magazine 147, 42–58.

Tsunogae, T., Osanai, Y., Toyoshima, T., Owada, M., Hokada, T., Crowe, W.A., 1999. Metamorphic reactions and preliminary *p–T* estimates of ultrahigh-temperature mafic granulite from Tonagh Island in the Napier Complex, East Antarctica. Polar Geoscience 12, 71–86.

Tsunogae, T., Santosh, M., Osanai, Y., Owada, M., Toyoshima, T., Hokada, T., 2002. Very high-density carbonic fluid inclusions in sapphirine-bearing granulites from Tonagh Island in the Archean Napier Complex, East Antarctica: implications for CO_2 infiltration during ultrahigh-temperature (T > 1,100 °C) metamorphism. Contributions to Mineralogy and Petrology 143, 279–299.

Tsunogae, T., Santosh, M., Dubessy, J., Osanai, Y., Owada, M., Hokada, T., Toyoshima, T., 2008. Carbonic fluids in ultrahigh-temperature metamorphism: Evidence from Raman spectroscopic study of fluid inclusions in granulites from the Napier Complex, East Antarctica. Geological Society, London, Special Publications, vol. 308, pp. 317–330.

Tsunogae, T., Liu, S.J., Santosh, M., Shimizu, H., Li, J.H., 2011. Ultrahigh-temperature metamorphism in Daqingshan, Inner Mongolia Suture Zone, North China Craton. Gondwana Research 20, 36–47.

White, R.W., Powell, R., Holland, T.J.B., Worley, B.A., 2000. The effect of TiO_2 and Fe_2O_3 on metapelitic assemblages at greenschist and amphibolite facies conditions: mineral equilibria calculations in the system K_2O-FeO-MgO-Al_2O_3-SiO_2-H_2O-TiO_2-Fe_2O_3. Journal of Metamorphic Geology 18, 497–511.

White, R.W., Powell, R., Clarke, G.L., 2002. The interpretation of reaction textures in Fe-rich metapelitic granulites of the Musgrave Block, central Australia: constraints from mineral equilibria calculations in the system K_2O-FeO-MgO-Al_2O_3-SiO_2-H_2O-TiO_2-Fe_2O_3. Journal of Metamorphic Geology 20, 41–55.

White, R.W., Powell, R., Clarke, G.L., 2003. Prograde metamorphic assemblage evolution during partial melting of metasedimentary rocks at low pressures: migmatites from Mt Stafford, Central Australia. Journal of Petrology 44, 1937–1960.

White, R.W., Powell, R., Holland, T.J.B., 2007. Progress relating to calculation of partial melting equilibria for metapelites. Journal of Metamorphic Geology 25, 511–527.

Zhang, H., Li, J.H., Liu, S.J., Li, W., Santosh, M., Wang, H., 2012. Spinel + quartz-bearing ultrahigh-temperature granulites from Xumayao, Inner Monglia Suture Zone, North China Craton. Geoscience Frontiers 3, 603–611.